Dynamic response of damaged precast bridge girders

Bridge Maintenance, Safety, Management, Digitalization and Sustainability – Jensen, Frangopol & Schmidt (eds)

Dynamic response of damaged precast bridge girders

D. Sabia, A. Quattrone, F. Tondolo & P. Savino
Department of Structural, Geotechnical and Building Engineering, Politecnico di Torino, Torino, Italy

ABSTRACT: This paper presents a comprehensive dynamic test campaign conducted on pre-stressed concrete bridge beams sourced from a 50-year-old decommissioned viaduct in Turin, Italy, as part of the BRIDGE|50 research project. Individual beams were subjected to dynamic testing to assess the impact of varying levels of damage on their dynamic properties. Vibration data was collected before applying static loads, after reaching the first cracking condition, and after reaching maximum load capacity, and analysed to identify principal modal components. The findings underscore the correlation between damage progression and dynamic response, demonstrating the effectiveness of vibration tests in detecting and tracking damage evolution. Specifically, this study presents the experimental results pertaining to the tested I-shape beams.

1 INTRODUCTION

The vibration-based methods are one of the most widely adopted diagnostic tools in the field of structural monitoring of infrastructures. Vibration-based methods are widely applied in structural health monitoring techniques to follow the evolution of structural integrity, due to the direct dependence between the dynamic behaviour and the structural stiffness. Moreover, their appeal has increased due to the ease of managing the continuous streaming of large amount of data and inferring information by means of data mining algorithms. In literature, several studies report the results of experimental dynamic investigations on beam-like pre-stressed structures, focusing on their use as symptoms of the onset of damage or the evolution of deterioration over time (Quat-trone et al. 2012, Guiglia et al. 2014). For instance, a shift in the modal properties of a bridge can indicate variations in the stiffness or mass distributions, which can be caused by structural damages, modifications of constrain condition or the deterioration of the mechanical properties of the materials (Demarie et al. 2019).

However, these alterations can be challenging to be discerned in service condition due to the concurrent influences of multiple factors. The identification of modal parameters is affected by several noise sources and errors in the analyses process. Additionally, the influence of the variation of temperature and traffic conditions can influence the dynamic response of the structure, complicating the detection of stiffness-related variations induced by damages.

A continuous monitoring of these parameters can confirm the occurrence of even small variations, reducing the influence of error sources, highlighting the possible occurrence of damages. Consequently, conducting controlled tests on structures approaching the end of their service life can contribute significantly to provide more precise definitions of sensitivity limits and thresholds applicable to permanent monitoring systems.

The BRIDGE|50 research project, started in 2020, aims at deeply investigate the behaviour of aged bridge girders at the end of their service lives (Biondini et al. 2021). The research activities will be devoted to accurately investigate the structural performances and characterize the material properties of a representative portion of a viaduct dismantled after 50 years of service life, namely 25 prestressed concrete beams, 4 box girders and 2 pier caps.

The girders are tested in a controlled environments up to failure to determine their ultimate resistance. The dynamic tests have been performed adopting the simply supported configuration

DOI: 10.1201/9781003483755-413

simulating the original structural scheme. Vibrations have been collected before the execution of the static tests, in intermediate cracked state and at the end of static tests, after the application of the ultimate loading condition. The aim is to estimate the influence of the structural damage on the dynamic characteristics of the beams. Moreover, controlled damages are applied to a subset of beams by cutting strands at different locations. In this paper the results of the dynamic test campaign on a set of 8 I-shaped beams are reported.

2 THE CORSO GROSSETO VIADUCT

The Corso Grosseto viaduct was built in 1970. It was originally constituted by 90 concrete decks having variable spans, from 16 m to 24 m, and a total length of 1400 m (Figure 1). Each deck was composed of 10 precast prestressed concrete I-beams and 2 external precast prestressed concrete U-beams, simply supported at piers, and connected transversely by 3 equally spaced diaphragms and, on the top, by a 0.14 m concrete slab (Figure 2). A set of 25 prestressed concrete beams constituting the decks have been dismounted and collected in a testing area, where a bench test has been realized to perform both static and dynamic tests. The collected structural elements belong to the first four decks of the southern part of the viaduct, highlighted in green in Figure 2-a. The technical drawings of the I-beams cross section and the on-site casted slab, object of the present work, are shown in Figure 2 - b.

Figure 1. Corso Grosseto viaduct before the dismantling.

3 STATIC TEST CAMPAIGN

According to the preliminary visual inspection carried out to map the presence of corrosion, cracks, and spalling, the beams have been classified in good structural condition (Table 1). The beams B07 and B08 have been damaged during the dismantling phases, when strands at the bottom flanges were cut. The B07 had two strands cut on both sides of the lower flange, at distances of 3.7, 9.6, and two at 15.5 m from the end section. The B08 girder had four strands cut on one side at distances of 3.8 and 15.5 m. The B09 girder was damaged cutting 8 strands in two symmetrical positions 0.60 m from the midspan, resulting in a reduction of circa 40% of the total prestressing steel in the sections. The static test procedure consists in applying an increasing static load up to the reaching the ultimate load capacity by means of four hydraulic jacks. An

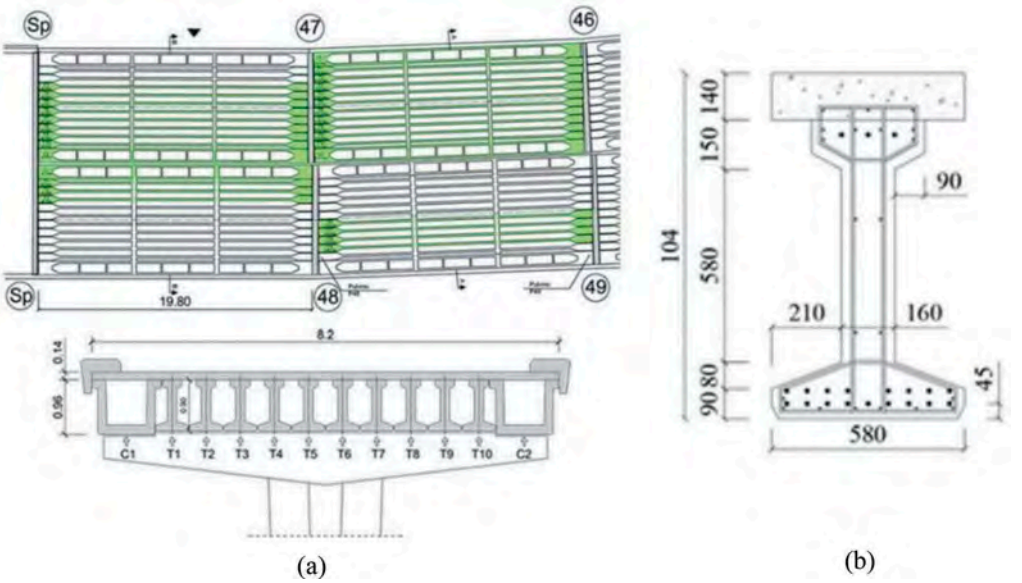

Figure 2. (a) Drawing of the first four decks of the southern part of the viaduct. In green, the beams collected. (b) The I-shaped beam cross section (measures in mm).

intermediate unloading phase was made to evaluate the residual prestressing load and the effects of the opening of the cracks on the dynamic parameters (Savino et al. 2023). The test on B02 beam has been performed in a three-point bending scheme (shear span 9.3 m), whereas a four-point scheme (shear span 6.5 m) was adopted for testing B05 to B11 girders, aimed at investigating the shear-bending interaction. The B11 was tested applying cyclic loading at three increasing load levels to explore the effects of cumulating damages. The B12 have been tested in four-point bending scheme adopting a shear span of 4 m. The beams have been loaded up to reach the ultimate condition highlighting a brittle rupture due to the crushing of the upper slab. The principal results are summarized in Table 1. For each girder, the ultimate flexural strengths M_R is calculated in the rupture section considering the effects of the self-weight, the weight of the load application systems and the maximum force applied by the hydraulic actuators during the test.

Table 1. Results of the static tests.

Beam	Position in the deck	Type	Testing Scheme	Condition	M_R (kNm)
B02	B8-P47/46	I	3-Point	Undamaged	2012
B05	B7-P47/46	I	4-Point	Undamaged	2057
B06	B6-SP/47	I	4-Point	Undamaged	1907
B07	B6-P49/48	I	4-Point	Damaged (4 strands cut at- 1/3 span and at midspan)	1845
B08	B10-SP/47	I	4-Point	Damaged (4 strands cut at- 1/3 span)	2080
B09	B5-P47/46	I	4-Point	Damaged (8 strands cut at midspan)	1412
B11	B2-P47-46	I	4-Point	Undamaged. Cyclic loading	2111
B12	B1-P47/46	I	4-Point	Undamaged	1968

4 DYNAMIC TEST CAMPAIGN

The setup adopted for the dynamic test of the beams is constituted by a set of 10 uniaxial capacitive accelerometers, glued on the top slab, having a sensitivity of 1V/g. The test setup is showed in Figure 3. The acceleration signals were acquired at a 512 Hz sampling frequency for both ambient noise and impact hammer excitations. The impact tests were carried out by hitting the beams with an instrumented hammer in vertical direction in the halfway of two consecutive positions. Dynamic tests were performed by removing the load application systems from the upper slab to replicate as closely as possible the constraint conditions typical of a simply supported isostatic beam.

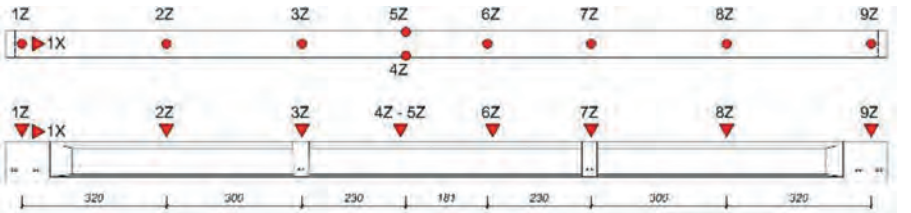

Figure 3. Dynamic test setup.

Dynamic tests were performed on all beams prior to the application of static loads (Phase 0). Whenever possible, the tests were repeated in an intermediate condition (Phase 1), and at the end of the static test (Phase 2), following the attainment of the ultimate failure load (Figure 4). The Phase 1 corresponds to the unloading condition, subsequent the reaching of the full cracked condition, identified in Table 2 as a fraction of the ultimate bending moment reached during the static tests calculated in the rupture section.

Table 2. Damage levels corresponding to phase 1 tests.

Specimen	M (kNm)	% M_R
B02	1453	72.2
B05	1278	62.2
B06	1208	63.4
B07	1243	67.3
B08	1306	62.8
B09	977	69.2
B11	1503	71.2
B12	N.P.	N.P.

4.1 *Experimental modal analysis*

The extraction of the principal modal components is performed evaluating the frequency response function (FRF) matrix with respect of the input given by means of the instrumented hammer. The element of FRF matrix $H_{k,j}(\omega)$ maps the input $F_k(\omega)$, applied at the k-th degree of freedom (DOF), and the output Y_j measured at the j-th DOF. In case of acceleration as output signals, the FRF matrix is expressed in the accelerance form (Ljung, 1999). The generic element of the accelerance matrix, expressed in terms of modal properties, is given by:

$$H_{j,k}(\omega) = \frac{\ddot{Y}(\omega)}{F_k(\omega)} = -\omega^2 \sum_{r=1}^{N} \frac{1}{m_r} \frac{{}^r\psi_j \, {}^r\psi_k}{\omega_r^2 - \omega^2 + 2i\omega\omega_r} \tag{1}$$

The FRF is a complex function which amplitude has a maximum at the resonant frequency. The magnitude of the modal coefficient is taken as the value of the imaginary part at resonance.

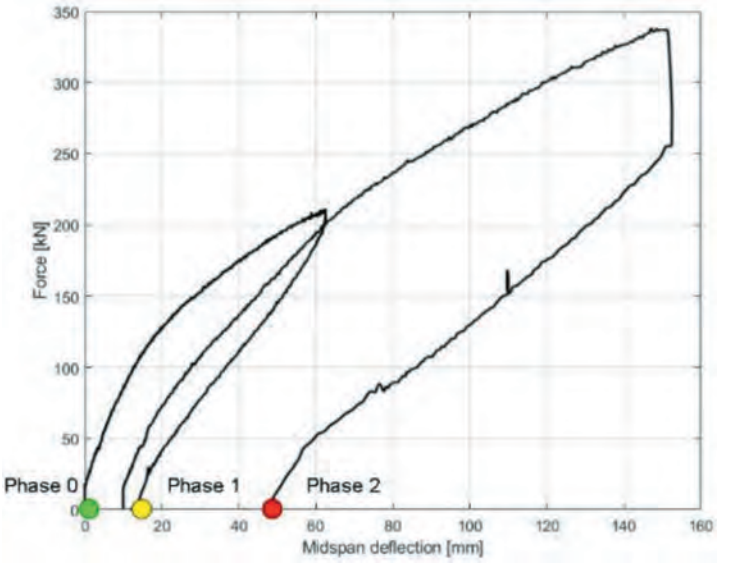

Figure 4. Force – midspan deflection. The dots indicate the phase test.

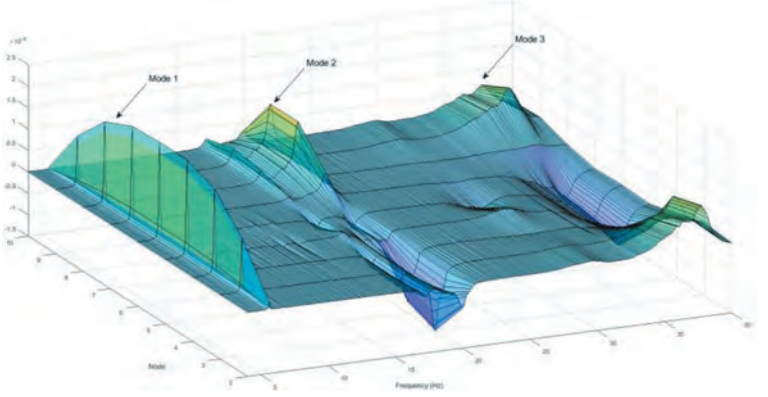

Figure 5. Example of mode shapes of the first three bending modes of the beam B06 – phase 0.

The sign is either positive or negative, considering the direction of the peak along imaginary axis. This implies that the phase angle is either 0° or 180°. After a preliminary analysis of the spectral content, the signals were pretreated by filtering out of the bandwidth [0 - 100 Hz], removing the trends. The FRFs have been estimated basing on each singular impulse acceleration data and then averaged for each hitting position. The first three modal components are clearly identified as shown by the example proposed in Figure 5. The mode shapes associated to these components correspond to the three main flexural modes of the beam. The modal coordinates are estimated by the imaginary part of the FRFs.

5 RESULTS OF THE DYNAMIC IDENTIFICATION

In this paragraph the results of the dynamic identification are proposed. The Table 3 reports the mean values of frequencies and damping estimated at the three phases for each beam. It can be noted that at the increase of the damage level correspond the reduction of the modal frequencies and the increasing trend of damping ratios.

Table 3. Mean modal frequencies and damping ratios.

		Phase 0			Phase 1			Phase 2		
		mode 1	mode 2	mode 3	mode 1	mode 2	mode 3	mode 1	mode 2	mode 3
B02	f (Hz)	5.49	19.38	36.44	5.28	18.88	36.34	4.78	18.58	32.69
	ξ(%)	0.37	0.84	2.18	0.48	0.81	2.19	0.55	1.00	2.22
B05	f (Hz)	5.47	19.72	36.88	5.31	19.50	35.75	5.03	19.28	32.66
	ξ(%)	0.34	0.80	1.94	0.40	0.74	1.68	0.95	2.16	2.03
B06	f (Hz)	5.60	19.86	37.21	5.47	19.48	36.17	5.01	18.50	33.62
	ξ(%)	0.36	1.30	0.85	0.40	1.33	0.91	0.63	1.06	1.57
B07	f (Hz)	5.58	19.83	35.22	5.48	19.36	34.91	5.01	19.09	33.84
	ξ(%)	0.39	0.65	1.77	0.39	0.68	1.99	0.42	1.30	2.14
B08	f (Hz)	5.61	20.35	38.25	5.41	19.58	37.08	4.83	18.33	33.85
	ξ(%)	0.29	1.46	1.32	0.31	1.04	1.57	0.43	1.06	1.57
B09	f (Hz)	5.35	19.80	35.08	5.16	18.59	33.50	4.34	18.22	30.47
	ξ(%)	0.31	0.81	1.73	0.35	0.66	2.70	0.51	0.67	1.69
B11	f (Hz)	5.53	19.72	36.72	5.22	18.88	33.72	-	-	-
	ξ(%)	0.35	0.82	2.99	0.47	0.73	2.92	-	-	-
B12	f (Hz)	5.56	19.88	34.97	-	-	-	4.69	16.94	32.78
	ξ(%)	0.33	0.63	2.49	-	-	-	0.50	0.57	2.32

NP: test not performed

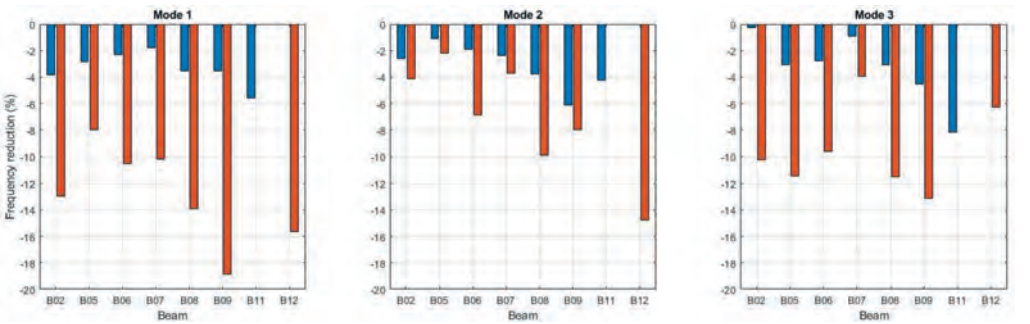

Figure 6. Relative modal frequencies reduction.

The Figure 6 shows the relative reduction of the modal frequencies at the different damage levels.

The following figures illustrate, as an example, the comparison between the mode shapes at different damage levels (phases 0, 1 and 2) for girder B08. It worth noting that small but noticeable differences can be observed with the increasing of damages. Similar results have been found for the other girders.

The reductions of the frequencies of the first mode vary in range of about 2-6% for Phase 1 tests and about 8-19% for Phase 2. The entities of these reductions are comparable to the findings reported in similar experimental campaign present in literature (Quattrone et al. 2012).

It can be noticed that the variation of the first and third modes for B11 in Phase 1 are considerably higher than the mean values obtained in the other samples. It seems indicating a noticeable effect of the diffusion of cracks induced by the application of a higher number of loading cycles at the intermediate level.

The girder B09, which was damaged cutting the 40% of the prestressing strands concentrated at midspan, showed the higher reduction at the ultimate level (Phase 2). The crack pattern of B09 observed at the end of the tests evidences a concentration of cracks in the midspan, where the rupture occurred. In Figure 8 the comparison with the girder B05 shows the spreader diffusion of cracks in case of absence of concentrated damages.

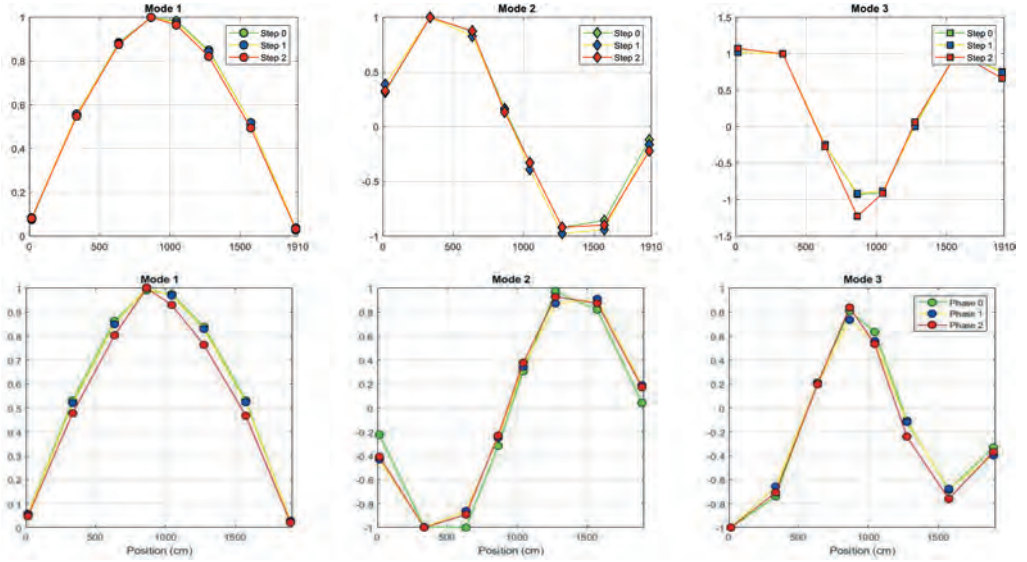

Figure 7. Modal shapes. top: girder B06. bottom: girder B09.

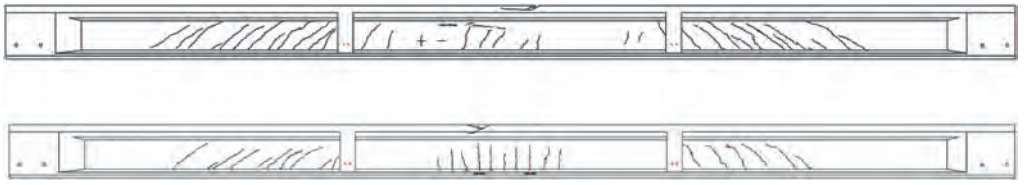

Figure 8. Cracks pattern after failure. top: girder B05. bottom: girder B09.

The Figure 9 highlights in red the domain of variation of the identified modal frequencies, normalized with respect of the undamaged condition, highlighting the wider scattering of the higher modal frequencies.

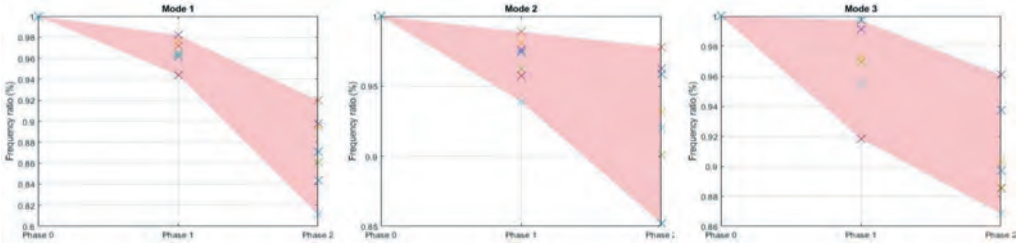

Figure 9. Domain of variation of the identified modal frequencies.

6 CONCLUSIONS

This work presents the results of the experimental dynamic campaign performed on a set of bridge girders dismounted after 50 years of service life. The tests are part of the BRIDGE|50 research project.

The girders have been characterized for different damage levels induced by static tests. The variation of the modal parameters has been observed and, albeit the small magnitude, the

variations of the structural condition are clearly detectable, confirming the capability of the dynamic structural identification to follow the evolution of damage. The experimental results here presented should be very useful in the field of permanent structural health monitoring. Future works will refine the estimation of damping ratio and the implementation of damage localization and quantification techniques.

ACKNOWLEDGEMENTS

BRIDGE|50 is a research project based on a research agreement among universities, public authorities, and private companies. Members of the Management Committee: S.C.R. Piemonte (President); Politecnico di Milano (Scientific Coordinator); Politecnico di Torino (Scientific Responsible of the Experimental Activities); Lombardi Engineering (Secretary); Piedmont Region; City of Turin; Metropolitan City of Turin; TNE Torino Nuova Economia; ATI Itinera & C.M.B.; ATI Despe & Perino Piero; Quaranta Group. BRIDGE|50 website: http://www.bridge50.org

REFERENCES

Biondini, F., Manto, S., Beltrami, C., Tondolo, F., Chiara, M., Salza, B., et al. BRIDGE|50 research project: Residual structural performance of a 50-year-old bridge. *Bridge Maintenance, Safety, Management, Life-Cycle Sustainability and Innovations – Proceedings of the 10th International Conference on Bridge Maintenaince, Safety and Management (IABMAS 2020)*.

Demarie G, Sabia D. A machine learning approach for the automatic long-term structural health monitoring, Structural Health Monitoring, 819–837 (2019).

Guiglia, M., Taliano, M.: Experimental analysis of the effective pre-stress in large-span bridge box girders after 40 years of service life. Engineering Structures 66 (1), 146–158 (2014)

Quattrone, A., Matta, E., Zanotti Fragonara, L., & Ceravolo, R., 2012. Vibration tests on dismounted bridge beams and effects of deterioration, *Journal of Physics: Conference Series*, 382(1).

Ljung, L.: System identification. Theory for users, Englewood Cliffs, NJ, Prentice Hall, (1999).

Quattrone, A., Sabia, D., Tondolo, F., Capacci, L., Lencioni, A., Legramandi, C.: Dynamic tests and modal identification of Corso Grosseto viaduct decks before the dismounting. Bridge Maintenance, Safety, Management, Life-Cycle Sustainability and Innovations. CRC Press (2021).

Sabia, D., Quattrone, A., Tondolo, F., Savino, P. Dynamic identification of damaged PC bridge beams. First Conference of the European Association on Quality Control of Bridges and Structures (EUROSTRUCT 2021), August 29 – September 1, 2021, Padua, Italy (2021).

Savino, P.; Tondolo, F.; Sabia, D.; Quattrone, A.; Biondini, F.; Rosati, G.; Anghileri, M.; Chiaia, B. 2023. Large-Scale Experimental Static Testing on 50-Year-Old Prestressed Concrete Bridge Girders. Applied Sciences 13(834): 1–22.